

## Elastic imaging in finely layered media

Wim J.F. van Geloven\* and C.P.A. Wapenaar, Centre for Technical Geoscience, Laboratory of Seismics and Acoustics, Delft University of Technology

### Summary

When a wave propagates through a bed of thin layers it gets dispersed and its reflection is accompanied by wavelet interference. These effects cause apparent AVA effects in seismic reflection data. Due to the bandlimitation of the seismic data, these AVA effects cannot be removed. However, by the application of generalized inverse wave propagators and a spatial bandlimitation filter, these effects can be equalized. This method was already tested for acoustic inhomogeneous media. We give here an extension of this method to elastic media. This extension also generalizes the theory.

### Introduction

The relation between amplitude versus offset observed in seismic data and the angle dependent reflectivity in a targetzone is complicated by many factors. These factors can be reflection related (thin bed tuning, reflector curvature), propagation related (geometrical spreading, transmission or anelastic losses) or acquisition related (geophone coupling, source receiver directivity).

In this abstract we will discuss the reflection and propagation related *apparent* AVA- (amplitude versus angle) effects due to elastic fine-layering. It is well known that the relation between the AVA-effects becomes complicated when the layer thickness becomes smaller than half the seismic wavelength [4]. These fine-layering effects cannot be removed due to the bandlimitation of the seismic wave. This means that the Zoeppritz equations that will be applied in the process of inversion will predict other AVA behaviour.

To alleviate this problem, in [1, 8] methods are discussed that can equalize the apparent AVA-behaviour in acoustic media. In this paper we discuss a generalization of the method to elastic media.

### Apparent AVA-effects of fine-layering

The apparent AVA-effects due to fine-layering can be subdivided into propagation related effects and reflection related effects. The propagation through a package of thin layers is accompanied by wavelet *dispersion*, the reflection by wavelet *interference*. These effects can be viewed as separate mechanisms as can be viewed in the formulation of the forward model.

The plane wave reflection response of a horizontal layered

medium, including all internal multiples can be written as

$$\tilde{\mathbf{P}}^-(p, z_0, \omega) = \int_{z_0}^{\infty} \tilde{\mathbf{W}}_g^-(p, z_0; z, \omega) \hat{\mathbf{R}}^+(p, z) \tilde{\mathbf{W}}_g^+(p, z; z_0, \omega) S^+(\omega) dz. \quad (1)$$

All boldfaced terms in this formulation are  $2 \times 2$ -matrices, where each element denotes a specific conversion. For example,  $\tilde{\mathbf{P}}^-(p, z_0, \omega)$  represents the decomposed multicomponent reflection data at the surface  $z_0$  in the  $p - \omega$  domain and is defined by

$$\tilde{\mathbf{P}}^-(p, z_0, \omega) = \begin{pmatrix} \tilde{P}_{PP}^- & \tilde{P}_{PS}^- \\ \tilde{P}_{SP}^- & \tilde{P}_{SS}^- \end{pmatrix}. \quad (2)$$

The operators  $\tilde{\mathbf{W}}_g^\pm$  are the generalized primary propagators [2, 5] which describe the plane wave transmission responses of the finely layered medium, including all internal reflections, causing dispersion hence, they account for the propagation related apparent AVA-effects of fine-layering.

The reflection of a package of thin layers is accompanied by wavelet interference, that depends on the angle as well. This can be explained with the aid of Figure 1, where two plane waves are shown that illuminate an acoustic medium with two different angles. The circular frequency of these waves is chosen to be the same. The vertical wavelength of these waves is therefore different and hence we can conclude that the medium is measured with two different gauges. Thus, the interference effects are different for distinct angles. Therefore we have to make the vertical wavelength constant as can be seen in Figure 2, which means that for different illumination

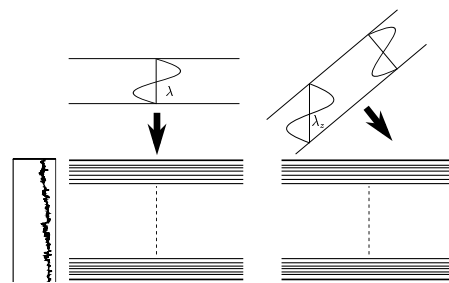


Fig. 1: Horizontally layered medium: Different angles  $\phi$ , same angular frequency  $\omega$

## Improved AVA imaging

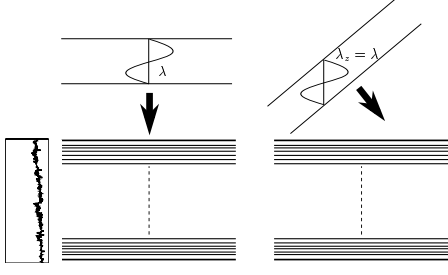


Fig. 2: Horizontally layered medium: Different angles  $\phi$ , same vertical wavelength  $\lambda_z$

angles we will use waves with different frequency content. It has to be remarked though that this wavelength criterion has no meaning for converted waves in elastic media. We have to use a generalized criterion that will be formulated in the next section.

### Compensating for the fine-layering effects

The first step in true amplitude migration is a downward extrapolation. To compensate for the angle dependent dispersion due to fine-layering, generalized primary inverse wave-propagators [7] are used in the redatuming step

$$\tilde{\mathbf{P}}^-(p, z, \omega) = \tilde{\mathbf{F}}_g^-(p, z; z_0, \omega) \tilde{\mathbf{P}}^-(p, z_0, \omega) \tilde{\mathbf{F}}_g^+(p, z_0; z, \omega). \quad (3)$$

The operator  $\tilde{\mathbf{F}}_g^\pm$  is the inverse of  $\tilde{\mathbf{W}}_g^\pm$ . Wapenaar et al. in [7] discuss how to compute this inverse operator in a stable manner. We remark again that each term of the latter equation is a  $2 \times 2$ -matrix. Each element, see also equation (2), of the redatumed matrix  $\tilde{\mathbf{P}}^-(p, z, \omega)$  is imaged separately.

The actual imaging step for each wave-conversion type is given by

$$\langle \tilde{R}_{\alpha,\beta}^+(p, z) \rangle = \frac{\mathcal{C}_{\alpha,\beta}(p, z)}{\pi} \Re \int_{\omega_1(p,z)}^{\omega_u(p,z)} \frac{\tilde{P}_{\alpha,\beta}^+(p, z, \omega)}{S_\beta(\omega)} d\omega, \quad \alpha, \beta = S, P. \quad (4)$$

The subscripts  $\alpha$  and  $\beta$  stand for the wavetype, which can be P or S. The factor  $\mathcal{C}_{\alpha,\beta}(p, z)$  and the limits of integration are defined as

$$\mathcal{C}_{\alpha,\beta}(p, z) = \frac{\cos \bar{\phi}_\alpha(p, z)}{\bar{c}_\alpha(z)} + \frac{\cos \bar{\phi}_\beta(p, z)}{\bar{c}_\beta(z)}, \quad (5)$$

$$\omega_l(p, z) = k_1 / \mathcal{C}_{\alpha,\beta}(p, z), \quad (6)$$

$$\omega_u(p, z) = k_2 / \mathcal{C}_{\alpha,\beta}(p, z), \quad (7)$$

$$\cos \bar{\phi}_\alpha(p, z) = \sqrt{1 - \bar{c}_\alpha^2(z) p^2}. \quad (8)$$

From these equations we can see that the limits of the integration vary with the wave-type, depth and ray-parameter. Furthermore

$\bar{c}_\alpha$  defines the  $\alpha$ -wave velocity. Optimally this is the exact velocity, practically it is chosen to be the macro-model velocity. How close  $\bar{c}_\alpha$  should be to the actual velocity is still under discussion. The wavenumbers  $k_1$  and  $k_2$  can be chosen arbitrarily as long as  $\omega_u$  and  $\omega_l$  do not exceed the bandlimits that are defined by the input source for the specific wavetype, given by  $S_\beta(\omega)$ .

As mentioned in the previous section the depth and angle dependent limits of integration of equation (4) yield that we measure the medium with the same gauge. For the simplified situation of ‘primaries only’ and a homogeneous macro model velocity, we can prove, by substituting equations (1) and (3) in (4), with the new limits of integration, that

$$\langle \tilde{R}_{\alpha,\beta}^+(p, z) \rangle = \int_{z_0}^{\infty} b(z - z') \tilde{R}_{\alpha,\beta}^+(p, z') dz', \quad (9)$$

or in the vertical wavenumber domain

$$\langle \tilde{R}_{\alpha,\beta}^+(p, k_z) \rangle = \check{b}(k_z) \tilde{R}_{\alpha,\beta}^+(p, k_z), \quad (10)$$

where  $\check{b}$  is a bandpass-filter of the form

$$\check{b}(k_z) = \begin{cases} 1 & \text{for } k_1 < |k_z| < k_2, \\ 0 & \text{elsewhere.} \end{cases} \quad (11)$$

From these equations we can conclude that the imaged reflectivity section  $\langle \tilde{R}_{\alpha,\beta}^+(p, z) \rangle$  is a band-filtered version of the true reflectivity section  $\tilde{R}_{\alpha,\beta}^+(p, z)$ , since the imaged reflectivity section is convolved with an *angle-independent* spatial wavelet  $b(z)$ . For this reason the apparent AVA-effects due to interference are compensated. A second noteworthy aspect is that the filter is of unit-amplitude. In [8] a complete derivation of these results is given.

### Examples

In this section, we shall corroborate the results of the previous section with some examples. In Figure 3 the P-wave and S-wave velocities are shown that are used to model the plane wave reflection response. The density in the medium is kept constant at a value of 2000 kg/m<sup>3</sup>. The plane wave reflection response of each specific conversion type, including all multiple reflections, is shown in the  $\tau - p$  domain in Figure 4. This result is generated by an elastic reflectivity method. It should be remarked that, since we used flux-normalized operators, the SP sections equal PS sections and therefore are omitted. The bandlimited reflectivity, computed from the well-log, is shown in Figure 5. This section serves as a reference section for our migration experiments.

The reflectivity image of a migration taking into account the effects of the fine layering is shown in Figure 6 (the reflectivity image of a normal migration is not displayed). The macro model velocity  $\bar{c}_\alpha$  that is used to replace the true velocity in the imaging

## Improved AVA imaging

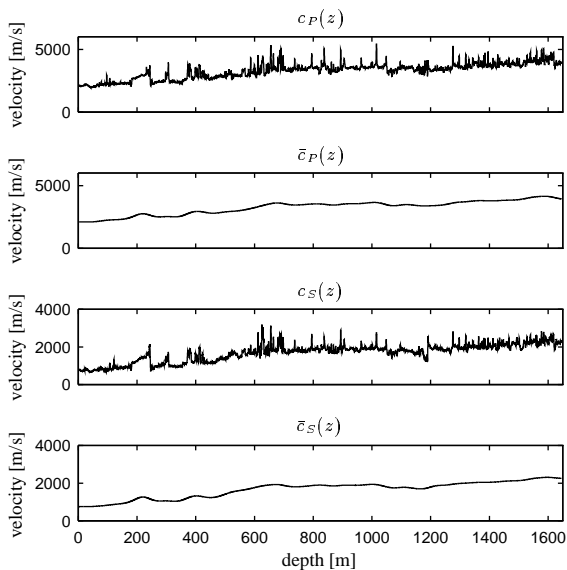


Fig. 3:  $P$ - and  $S$ -wave velocities used in the forward modelling scheme, with smoothed logs that serve as background model in the imaging step.

step (eqns. (4-8)) is shown in Figure 3. In Figure 7 the differences in the reflectivity images of a normal migration and the migration of Figure 6 with the reference section of Figure 5 are plotted. We can conclude that the latter section contains less differences with the reference section, thus that the apparent, propagation and reflection related AVA-effects are compensated.

### Conclusions

We have discussed an extension to the elastic case of a method that compensates for the propagation related and reflection related apparent AVA-effects. This method was already proven, within the context of the used modelling method, for acoustic media in one and two dimensions. In this paper, we have given an extension of this method to elastic media. By application of the generalized inverse elastic wave-propagators we have taken into account all angle dependent dispersion, i.e. the propagation related effects. Furthermore, we have shown that the imaging in elastic media with varying frequency limits yields a bandfiltered version reflectivity with no apparent angle dependence induced by the migration. In this way the effects of interference are compensated.

Points of interest in the future will be the sensitivity of the method due to errors in the estimated background velocity and the application of the method to real field examples.

### Acknowledgement

The work reported here was supported under a grant from the Dutch Science Foundation STW (DTN 44.3547)

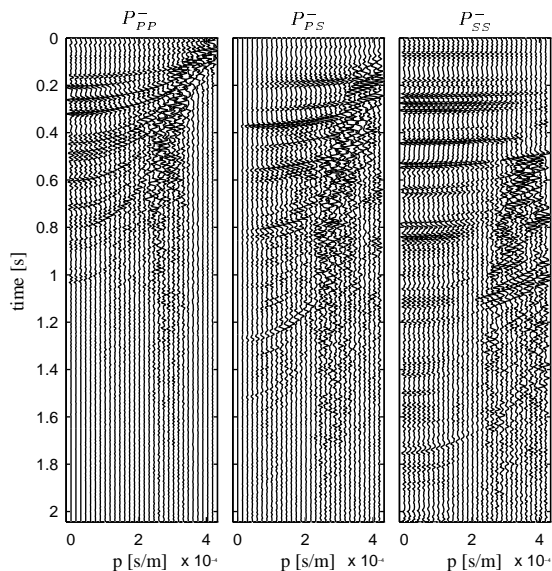


Fig. 4: Plane wave reflection response of  $P_{PP}^-$ ,  $P_{PS}^-$ ,  $P_{SS}^-$  including all internal multiples;  $P_{PS}^-$  equals  $P_{PS}^-$  because of the flux-normalization and is therefore omitted.

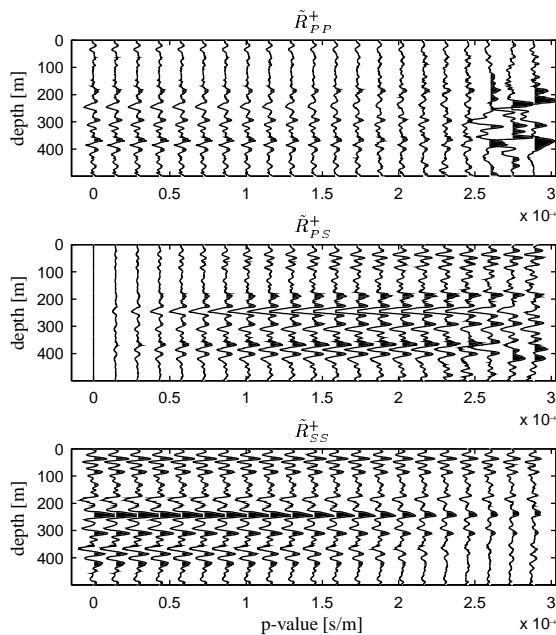
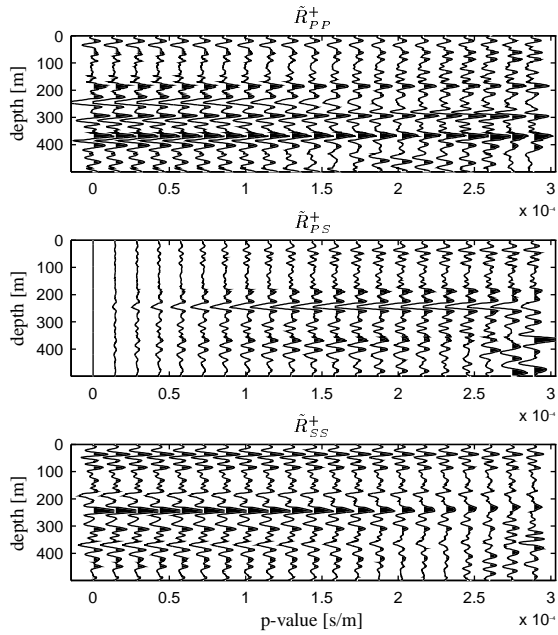


Fig. 5: Bandlimited reflectivity sections, which serve as a reference for the migration experiments.

## Improved AVA imaging



**Fig. 6:** Reflectivity sections in the  $p - z$  domain as a result of a migration with generalized operators and with a fixed spatial bandwidth

### References

- [1] Geloven, W.J.F., and Wapenaar, C.P.A., 1996, Improved AVA imaging in laterally varying media: 66th annual SEG meeting, Denver.
- [2] Hubral, P., Treitel, S., and Gutowski, P.R., 1980, A sum autoregressive formula for the reflection response: *Geophysics*, **45**, 1697-1705.
- [3] O'Doherty, R.F., and Anstey, N.A., 1971, Reflections on amplitudes: *Geophys. Prosp.*, **19**, 430-458.
- [4] Ostrander, W.J., 1984, Plane-wave reflection coefficients for gas sands at nonnormal angles of incidence: *Geophysics* **49**, 1637-1648.
- [5] Resnick, J.R., Lerche, I., and Shuey, R.T., 1986, Reflection, transmission, and the generalized primary wave: *Geophys. J. Roy. Astr. Soc.*, **87**, 349-377.
- [6] Walden, A.T., and Hosken, J.W.J., 1985, An investigation of the spectral properties of primary reflection coefficients: *Geophys. Prosp.*, **33**, 400-435.
- [7] Wapenaar, C.P.A., and Herrmann, F.J., 1996, True amplitude migration taking fine-layering into account: *Geophysics*, **61**, 804-814.

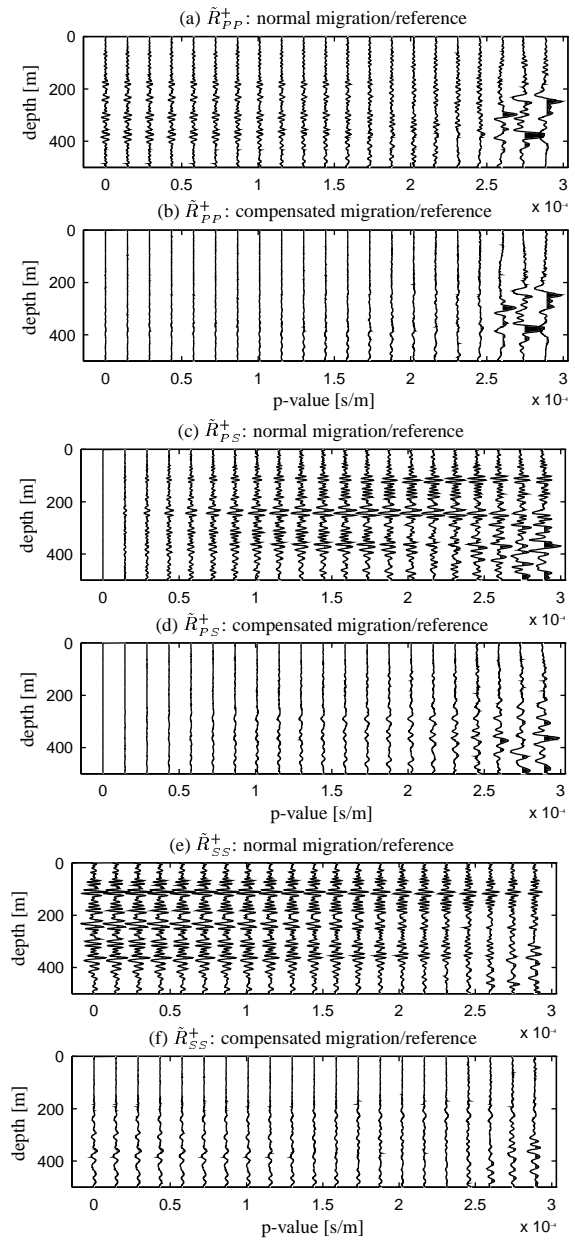


**Fig. 7:** Differences for  $\tilde{R}_{PP}^+$ ,  $\tilde{R}_{PS}^+$  and  $\tilde{R}_{SS}^+$  of the reference section of Figure 5 in the  $z - p$  domain with a normal migration: subfigures (a,c,e), and the migration of Figure 6: subfigures (b,d,f).

- [8] Wapenaar, C.P.A., W.J.F. van Geloven, T.S. van der Leij and A.J. van Wijngaarden, 1997, AVA and the effects of fine-layering, *Geophysics* (submitted).